

Causal interactions from proteomic profiles: molecular data meets pathway knowledge

Özgün Babur^{1,2,*}, Augustin Luna³, Anil Korkut⁴, Funda Durupinar², Metin Can Siper², Ugur Dogrusoz⁵, Joseph E. Aslan⁶, Chris Sander³, and Emek Demir^{1,2}

¹Department of Molecular and Medical Genetics, Oregon Health and Science University, 3181 SW Sam Jackson Park Rd, Portland, OR 97239, USA

²Computational Biology Program, Oregon Health and Science University, 3181 SW Sam Jackson Park Rd, Portland, OR 97239, USA

³cBio Center for Computational and Systems Biology, Dana-Farber Cancer Institute, and Department of Cell Biology, Harvard Medical School, Boston, MA 02215, USA

⁴Department of Bioinformatics and Computational Biology, The University of Texas MD Anderson Cancer Center, Houston, TX 77030, USA

⁵Computer Engineering Department, Bilkent University, Ankara 06800, Turkey

⁶Knight Cardiovascular Institute, Oregon Health and Science University, 3181 SW Sam Jackson Park Rd, Portland, OR 97239, USA

*babur@ohsu.edu

ABSTRACT

Measurement of changes in protein levels and in post-translational modifications, such as phosphorylation, can be highly informative about the phenotypic consequences of genetic differences or about the dynamics of cellular processes. Typically, such proteomic profiles are interpreted intuitively or by simple correlation analysis. Here, we present a computational method to generate causal explanations for proteomic profiles using prior mechanistic knowledge in the literature, as recorded in cellular pathway maps. To demonstrate its potential, we use this method to analyze the cascading events after EGF stimulation of a cell line, to discover new pathways in platelet activation, to identify influential regulators of oncoproteins in breast cancer, to describe signaling characteristics in predefined subtypes of ovarian and breast cancers, and to highlight which pathway relations are most frequently activated across 32 cancer types. Causal pathway analysis, that combines molecular profiles with prior biological knowledge captured in computational form, may become a powerful discovery tool as the amount and quality of cellular profiling rapidly expands. The method is freely available at <http://causalpath.org>.

Introduction

Recent advances in proteomics have led to rapid expansion of applications and datasets, providing unprecedented opportunities for elucidating pathway mechanisms that link perturbations to observed changes¹. There are two types of approaches in this direction: (i) explaining data with known pathway relations, (ii) predicting new pathway relations using data; and they are not mutually exclusive. We and others have previously shown that combining general prior knowledge from pathway databases with context-specific proteomic observations is an excellent approach to infer context-specific active sub-mechanisms^{2,3}. In this manuscript, we exclusively focus on utilization of existing knowledge.

Recent methods for the utilization of existing pathway knowledge provide two major services: (i) mapping data onto networks to visualize the data and the related network at the same time, (ii) propagating the data over network relations to infer new genes/proteins that can be related to the observed changes on other proteins. PTMapper⁴ is an example for the first approach where proteomics data is mapped onto a network and enriched regions are selected. pCHIPS⁵ is an example of the second approach where proteomic changes are propagated downstream and transcription factor activities are propagated upstream to identify possible intermediary signaling paths. All these methods, while useful, provide vague explanations for the data because the methods lack mechanistically justified causal reasoning. Causality is an essential component for a data explanation model, as it introduces predictability in the system and opens up opportunities for developing alteration strategies for a desired change. Causality is often part of the methods that infer new pathway relations from omic data⁶⁻⁸. On the other hand, despite being highly desired, causality is much less emphasized while explaining data with known pathways.

A probabilistic causal relationship between two events, say from event *A* to event *B*, indicates the probability of *B* depends on the status of *A*, as described by Patrick Suppes⁹. While using this notion of causality can generate predictive models, it

does not tell if A causes B . For instance, there can be an event X that is causing both A and B , and this will still satisfy Suppes' formulation. To make the model predictive under an intervention scenario, Judea Pearl provides a reformulation: forcibly changing the status of A will change the probability of B ¹⁰. In a pathway inference case, using Pearl's causality requires the data to include perturbations because such a model cannot be accurately derived only from observational data when there are hidden variables. In the case of data explanation with existing pathways, using Pearl's causality means that the pathway relation should suggest a mechanism for how the change in A will lead to a change in B .

Such detailed mechanistic pathways are curated from the literature by several databases including Reactome¹¹, PANTHER Pathways¹², PhosphoSitePlus¹³, HumanCyc¹⁴, KEGG¹⁵ and NCI PID¹⁶. But the data in them, with the exception of PhosphoSitePlus, are not simple graphs as in protein-protein interaction databases or binary signaling databases, because such mechanistic details require a more complex ontology. This complexity poses a barrier to researchers due to lack of intuitive tools that process these complex structures and generate simple-to-use knowledge for causal reasoning.

We previously collaborated with other researchers for the development of a standard ontology for detailed mechanistic pathways, named BioPAX¹⁷. Most of the major pathway database developers were part of this effort and they adopted BioPAX as one of their data distribution formats. In another collaboration, we developed the database called Pathway Commons that integrates all publicly available human pathway data in BioPAX language, which now contains 22 data resources, making it the largest integration of human pathway databases supporting detailed mechanisms¹⁸. On top of these, we developed software tools for performing computations on BioPAX models, such as Paxtools¹⁹, BioPAX-pattern²⁰, and ChiBE^{21,22}. These developments greatly increased the accessibility of mechanistic pathways and created an opportunity for this study.

Here we present CausalPath—a new causal pathway analysis pipeline that generates explanations for the coordinated changes in proteomic and phosphoproteomic profiles using literature-curated mechanistic pathways. By carefully studying detailed models in Pathway Commons, we generate a library of graphical patterns that detect certain relationships between pairs of proteins. Then we identify the subset of the omic changes that are causally explainable by the relations that our graphical patterns detect. We render these explanations as an intuitive simplified network, but also link to the relevant detailed models and the related literature to establish a powerful analysis platform (Fig. 1). This approach, in essence, mimics the literature search of a biologist for relationships that explain their data. Automating this task enables asking multiple interesting questions that would be too time-consuming to do through manual curation. Since this process systematically considers hundreds of thousands curated mechanisms, it also is more comprehensive, unbiased, and more consistent in terms of the generated hypotheses.

Using this framework, we analyze several phosphoproteomic datasets including a mass spectrometry dataset from an EGF stimulation experiment on a cell line, large mass spectrometry datasets from two CPTAC projects (breast cancer and ovarian cancer), and all the RPPA datasets from the TCGA project.

Results

Design and properties of CausalPath

Two questions central to the CausalPath design are “What can explain a phosphopeptide change?” and “What can explain a total protein level change?”. Kinase-substrate databases and transcription factor-target databases can help answer these questions respectively. However, they are limited in size, and too simplistic for a comprehensive causal reasoning. Many kinases, phosphatases and transcription factors function as parts of molecular complexes, which are often described in the literature and curated by the pathway databases that support detailed mechanistic models. Such models can use multi-level nesting, generalizations such as homologies, and non-trivial mechanisms such as the use of small molecule messengers. To detect structures that imply causal relations between proteins in the Pathway Commons database, we used the BioPAX-pattern software, and manually curated 12 graphical patterns (see Supplementary Doc). Searching for these patterns in Pathway Commons generated 20032 phosphorylations, 2767 dephosphorylations, 4921 expression upregulations, and 811 expression downregulations as signed and directed binary relations. To increase coverage, we added relations from several other databases (PhosphoNetworks²³, IPTMNet²⁴, TRRUST²⁴ and TFactS²⁵) which are not in Pathway Commons, and increased our numbers to 24433, 2767, 9060, 2961, respectively. Numbers show that detailed pathway databases leave much room for improvement in terms of expression relations, but they provide rich data for the explanation of phosphorylation changes.

A potential causal relation is a chain of knowledge fragments that collectively support the hypothesis of “one proteomic change is the cause of another proteomic change”. As an example, consider a platelet activation study that detects a set of proteomic changes. The chain of items below supports the hypothesis of one change causing the other.

1. NCK2-pY110 is increased in response to platelet activation.
2. Y110 is an activating phosphorylation site of NCK2.
3. NCK2 is part of a complex that can phosphorylate MAPK14 at S180 and Y182.
4. MAPK14-pS180-Y182 is increased in response to platelet activation.

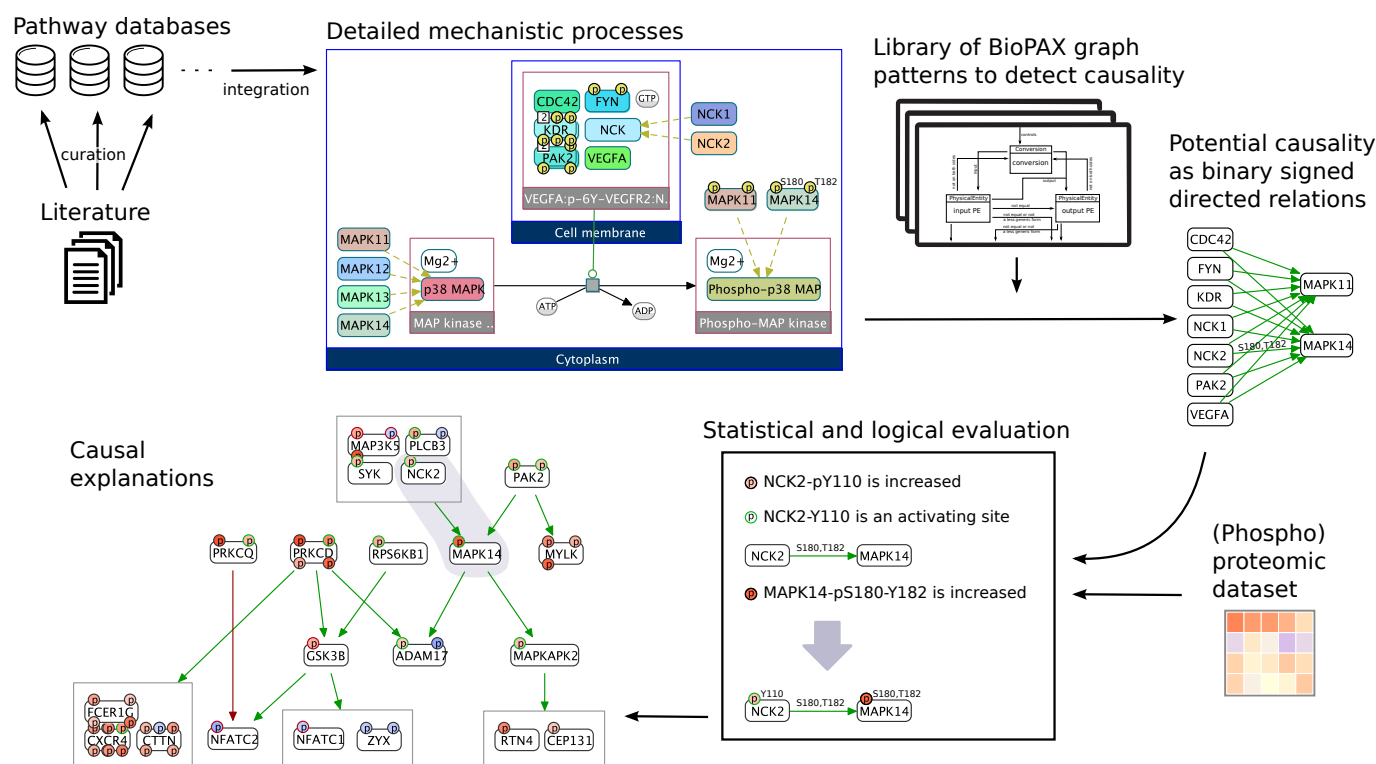


Figure 1. Design of CausalPath. The final logical network shows the 20 relations in platelet activation analysis results. For a description of graph notation please see Figure 2C. We omit phosphorylation site locations while rendering the result network for complexity management. These are revealed to the user upon clicking on nodes or edges in our interactive tools.

Items 1 and 4 come from the proteomics profile, and items 2 and 3 come from the literature, and pathway databases. The hypothesis that links all these data is that the increase in phospho-NCK (NCK2-pT110) caused an increase in its activity of phosphorylating MAPK14, hence an increase in MAPK14-pS180-T182 (Fig. 1). Alternative to comparing control and test samples, a causality network can be generated based on the correlations of measurements in a cohort. In that case, we replace items 1 and 4 with an observed correlation, e.g. “NCK2-pT110 is positively correlated with MAPK14-pS180-T182”, for a correlation-based causality hypothesis.

$$c_{source} e_{source} s_{relation} c_{target} = 1 \quad (1)$$

To formalize and generalize this example of causal interaction detection, we can formulate it with a logical equation (Eq. 1), where c represents the change direction of the gene features, e represents the effect of the source feature on its activity, and s represents the sign of the pathway relation, where $c, e, s \in \{-1, 0, 1\}$. Four terms in the equation corresponds to the four items in the example. The effect of source feature e_{source} is 1 in the case of total protein and activating phosphorylation, and it is -1 in the case of inactivating phosphorylation. In the case of correlation-based causality, the term $c_{source}c_{target}$ in Eq. 1 is replaced with the sign of the significant correlation between source and target features.

As an optional step of the analysis, CausalPath can perform 4 types of statistical significance calculations on the generated explanations. The first one is for the size of the produced explanations. If the proteomic data is heavily shaped by the known relations, then we will have many explanations. Other statistics are calculated for each protein in the analysis by evaluating the size of proteomic changes observed on their downstream: (i) changes explainable by either activation or inhibition of the upstream protein, (ii) changes explainable by activation, (iii) changes explainable by inhibition. While any of these statistics do not invalidate the results when they are insignificant, they provide additional information that can increase or decrease confidence for the explanations when significant. The null hypothesis for each of these cases is that the profiling data is independent from the network relations, which means a permutation of data labels will yield similar statistics. We assess the significances with data label randomization, and mark the significant proteins on the resulting network. The last two metrics do not apply to correlation-based cohort studies, but to control and test comparison-based studies.

We developed a new graph notation to represent explanations as a logical network, where nodes denote proteins and edges

denote causal relations (Fig. 2C). Node background is used for color-coding total protein change, while site-specific changes are shown with small circles on the nodes whose border colors indicate whether the site is activating/inhibiting. If additional omic data such as RNA expression, DNA copy number, or mutation status are available, we include them for integrated visualization, using small circles displaying specialized letters. Binary causal relations are represented with edges— green representing positive, red representing negative, phosphorylations with solid edges and transcriptional regulations with dashed edges. When significance calculation results are available, they are represented on the protein borders, using a bold border when downstream of a protein is significantly large, green border when downstream indicates the protein is activated, and red border when downstream indicates the protein is inactivated. If both the activation-indicating and inhibition-indicating downstreams are significantly large, then a dark yellow color is used instead. We use topology grouping while rendering result networks, which means we group the proteins with the same network topology under compound nodes on the network for complexity management.

We provide CausalPath as an open source Java library, and also provide a web service for easy access to the method.

Analysis of platelet activation

We recently used a preliminary version of CausalPath to analyze quantitative changes in the phosphoproteome of blood platelets stimulated with the purinergic receptor agonist ADP²⁶. The aim of this study was to generate testable hypotheses regarding known and novel pathways that regulate platelet function. We identified 20 relations that causally explain correlated changes in 21 phosphopeptides (Fig. 1). One of these identified relations, phosphorylation of RTN4 (a BCL2L1 sequestration protein) at S107 by MAPKAPK2, was not previously described in the context of platelet activation, but suggested a link from MAPK14 (p38 MAPK) signaling to endoplasmic reticulum physiology and apoptotic signaling events that have central roles in the early events of platelet activation. To test this hypothesis put forth by CausalPath analysis, we examined the phosphorylation of RTN4 in activating platelets under control as well as MAPK14- and MAPKAPK2-inhibited conditions by Western blot and fluorescence microscopy. Ultimately, we verified that MAPK signaling specifically drives RTN4 phosphorylation in activating platelets²⁶. Accordingly, we demonstrated that CausalPath can generate novel, testable hypotheses for discovery.

Analysis of EGF stimulation on EGFR Flp-In cells

We used a recent EGF stimulation time series phosphoproteomic dataset⁸ to see if CausalPath can recapitulate known biology, and to understand its limits. This dataset contains 8 time points, where the first time point (0 min) is unstimulated cells. We compared each of the other time points to the first time point to see how the cellular signaling evolves over time (Supplementary Animation 1). Since the data is phosphopeptide-only and does not contain any observable change on EGF itself, we included EGF activation as an hypothesis to the analysis. Consistent with our expectations, in the initial time points, CausalPath detects many EGFR targets and relates them to EGFR phosphorylation and activation. Both EGF and EGFR downstream are significantly enriched with changes that indicate their activation. At the 5th time point (16 min), we observe an inhibitory feedback phosphorylation of EGFR explainable by MAPK1 and MAPK3 activity, which follows with the disappearance of EGF signaling. All the networks up to the 5th time point are significant in size ($p < 0.0001$). What is missing in these graphs is an explanation for MAPK1/3 phosphorylation. It is known that EGF signaling can activate MAPK1/3 through several steps and multiple paths, but none was captured. One reason is that we are using CausalPath in the most strict configuration, forcing phosphorylation positions in the literature to exactly match the detected sites in the phosphoproteomic data. When we slightly relax this constraint by allowing 2 amino acids difference in site locations, we detect that SHC1 and GAB1 phosphorylations can causally link EGF stimulation to MAPK3 phosphorylation (Supplementary Animation 2). Our review of slightly shifted sites indicates that the site locations in the literature do not always map to the sequence of the canonical protein isoform provided by UniProt. For instance, one source of inconsistency is whether to count the initial methionine on the protein which is often cleaved. Hopefully, new publications will more reliably map protein modification sites to UniProt. CausalPath option to slightly relax the site matching is useful for detecting those inconsistencies.

Analysis of CPTAC ovarian cancer dataset

Ovarian cancer is a form of gynecological cancer that was estimated to kill 14,240 women in USA in 2016²⁷. High-grade serous ovarian cancer (HGSOC) is a molecular subtype which was subject to a TCGA project that investigated HGSOC with several kinds of omic profiling on 489 patients²⁸. HGSOC is often characterized by TP53 mutation (~95% of cases), low rates of other mutations, and extensive DNA copy number alterations. Following this TCGA project, a recent CPTAC project performed proteomic and phosphoproteomic analysis on the 174 of the original TCGA ovarian cancer samples using mass spectrometry, providing measurements for 9,600 proteins from the 174 samples and 24,429 phosphosites from 6,769 phosphoproteins from 69 samples²⁹.

Using CausalPath on this dataset, we generated explanations for the observed correlations in terms of phosphorylation and expressional control relations. The resulting phosphorylation network contains 116 relations and the expression network

contains 249 relations when we use a 0.1 false discovery rate (FDR) threshold for correlations. Interestingly, while the size of the phosphorylation network is significantly large ($p < 0.0001$, calculated by data label randomization), we do not observe this for the expression network ($p = 0.6482$), suggesting that the data is shaped by known phosphorylations more than by known expressional controls. The most noticeable parts of the phosphorylation network include CDK1 and CDK2 downstream, MAPK1 and MAPK3 downstream, and several immune-related protein activities such as SRC family kinases, PRKCD, and PRKCQ (Fig. 2A).

It was puzzling, initially, to obtain radically different significance values for expressional relations compared to phosphorylations. This could be either due to the low quality of expressional relations, or due to the total protein measurements being a bad proxy for their RNA expression. To investigate this, we modified CausalPath to use TCGA RNAseq data instead of proteomic data as the target of expressional controls. We obtained 192 expressional relations that explain RNA measurements of 133 genes with proteomic changes of 89 transcription factors or their modulators (Supplementary Fig. 2). This time, number of resulting relations is significantly large ($p < 0.0001$) suggesting that proteomic change is not a very good proxy for RNA expression. Additionally, the downstream changes of 5 transcription factors (STAT1, NFKB1, MCM6, CBF and SPI1) are significantly large (0.1 FDR), promoting these factors as most influential for generating variance in ovarian cancer.

The correlation-based causal network provides hypotheses for the signaling network parts that are differentially active across samples, but it does not tell which parts are activated together or whether they align with previously defined molecular subtypes. The original TCGA study on HGSOC samples identifies four molecular subtypes based on RNA expression, termed as immunoreactive, differentiated, proliferative, and mesenchymal²⁸. To understand if there is a mapping from this network to the previously defined subtypes, we compared each subtype to all other samples but we were unable to generate results within 0.1 FDR threshold, probably due to the large proportion of missing values in the phosphoproteomic dataset. Then we tried to constrain the search space with the neighborhoods of some of the genes with differential measurements, and relax the FDR threshold at the same time for further exploration. 6 SRC family kinases (SFKs) have proteomic evidence for activation in the immunoreactive subtype, hence, we limited the search to the neighborhood of SFKs (SRC, FYN, LYN, LCK, HCK, and FGR), set FDR threshold to 0.2 for phosphoproteomic data, and identified 27 relations (Fig. 2B). The network identifies several human leukocyte antigen (HLA) system (the major histocompatibility complex (MHC) in humans) proteins at SRC family upstream, along with other genes regulating immune cell activation such as CD4, ITGA4, PTPRC, PTPRJ, PTPN1, and NCK1. On the network, we can track their signal going over SFKs to CD247 and FCER1G, immune response genes.

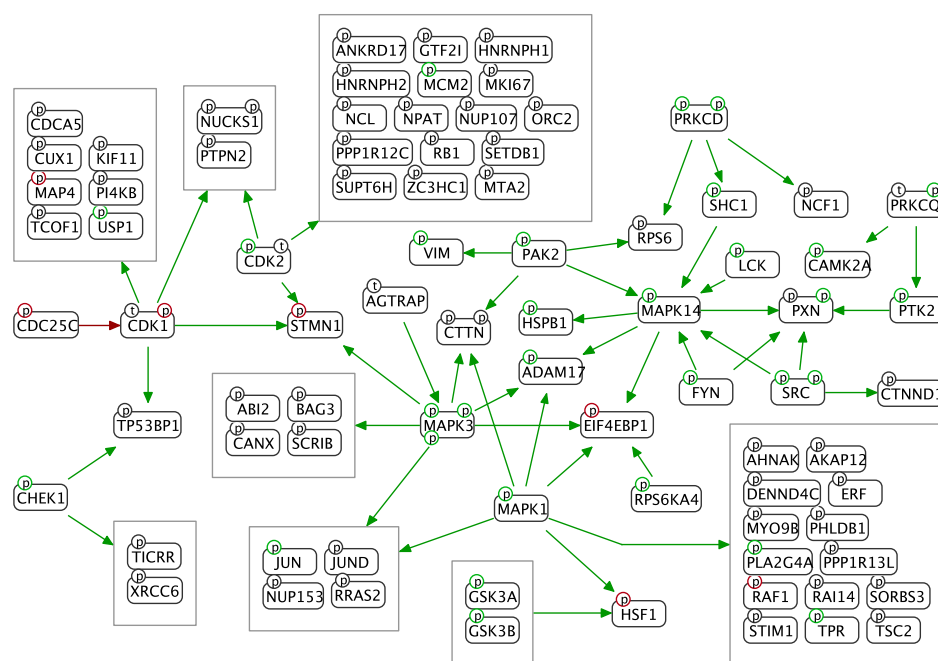
Analysis of CPTAC breast cancer dataset

Another CPTAC project produced proteomic and phosphoproteomic profiles for 105 of the original TCGA breast cancer samples with mass spectrometry³⁰. Unlike the ovarian cancer dataset, this dataset is rich in correlations, which can be explained by 2324 phosphorylation and 1497 expressional control relations. Similar to the ovarian cancer results, we detected the resulting phosphorylation network is significantly large ($p < 0.0001$) while the expression network is not ($p = 0.8070$), suggesting the known phosphorylation relations have a much higher impact on the proteomic correlations than known expressional relations. When we use TCGA RNAseq data instead of proteomic data for the targets of expressional relations, we detect 258 relations that explain RNA changes of 161 target genes by proteomic changes of 127 transcription factors or their modulators (Supplementary Fig. 4). This time, the size of the network is highly significant ($p < 0.0001$), with 7 transcription factors (STAT1, MCM5, ESR1, MCM6, GATA3, SOX10 and IL18) having targets enriched in the results (0.1 FDR).

For complexity management and to focus on the most interesting part of the phosphorylation network, we used a stricter FDR threshold of 0.001 and searched for regulators of known cancer proteins that could explain these correlations. We collected the so called “cancer genes” from databases OncoKB³¹ and COSMIC Cancer Gene Census³², and generated a subgraph with upstream neighbors of proteins related to those genes, which resulted in 205 relations with 98 cancer proteins controlled by 79 other proteins in breast cancer (Fig. 3A). Among 79 proteins we detected that MAPK14 was the most influential one, controlling 11 cancer proteins, followed by CDK2 controlling 10 cancer proteins on the network. Targeting CDK2 and other CDKs is an ongoing effort in cancer therapy with a challenge of toxicity^{33,34}. MAPK14 has conflicting reports on its anti- and pro-tumor activity³⁵. This complexity and toxicity is expected given that these proteins exert control over too many important proteins, the effect of targeting them will likely depend on the current state of their downstream proteins for each patient. A better strategy may be to direct research towards personalized treatments where patients are profiled for the activity of known cancer proteins and the relevant regulators are targeted. In such a setting, the causal relations we identified would be very useful to decide what to target, and how.

As a next step in the analysis, we compared the PAM50 expression subtypes of breast cancer to see if we could get causal explanations to their proteomic differences. We were again challenged by decreased sample sizes and missing values, but we detected that both luminal A and luminal B have significant differences from the basal-like subtype. This time, CausalPath results are not significant in terms of the overall network size ($p = 0.5184$), nevertheless, they indicate that ESR1 is significantly more active in luminal breast cancer while CDK1 is significantly more active in basal-like subtype, suggested by both their

A) Ovarian cancer correlation-based causal relations



C) Graph key

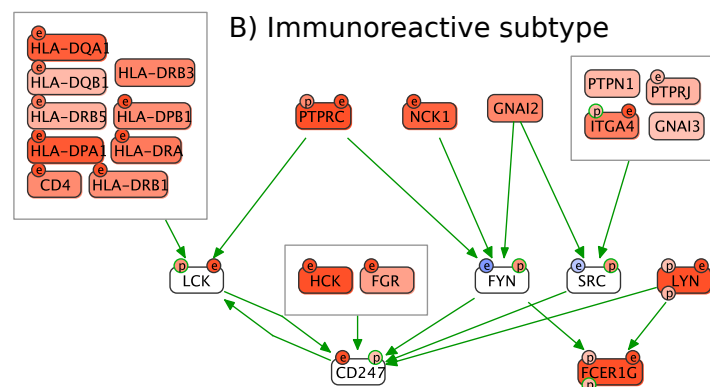
Graph elements

- SYMBOL A protein
- P A protein with a phosphorylation site
- P Activating phosphorylation site
- P Inactivating phosphorylation site
- t Total protein for correlation-based results
- e RNA expression
- C DNA copy number
- m Mutation status
- a Activity

Relations

- Phosphorylation
- Dephosphorylation
- - - - - Expression upregulation
- - - - - Expression downregulation

B) Immunoreactive subtype



Data change

- (for comparison-based results)
- Total protein increased
- Total protein decreased
- Gene/protein feature increased
- Gene/protein feature decreased

Significances

- Signif. downstream changes
- Downstream indicates activation
- Downstream indicates inhibition
- Downstream indicates both activation and inhibition

Figure 2. Results for CPTAC ovarian cancer. A) The largest connected component in correlation-based causality network. The complete network is in Supplementary Fig. 1. B) Immunoreactive subtype compared to all other samples, where we show RNA expression and DNA copy variation from corresponding TCGA datasets along with the CPTAC proteomic changes. C) Key for graph notation for causal explanations in all figures.

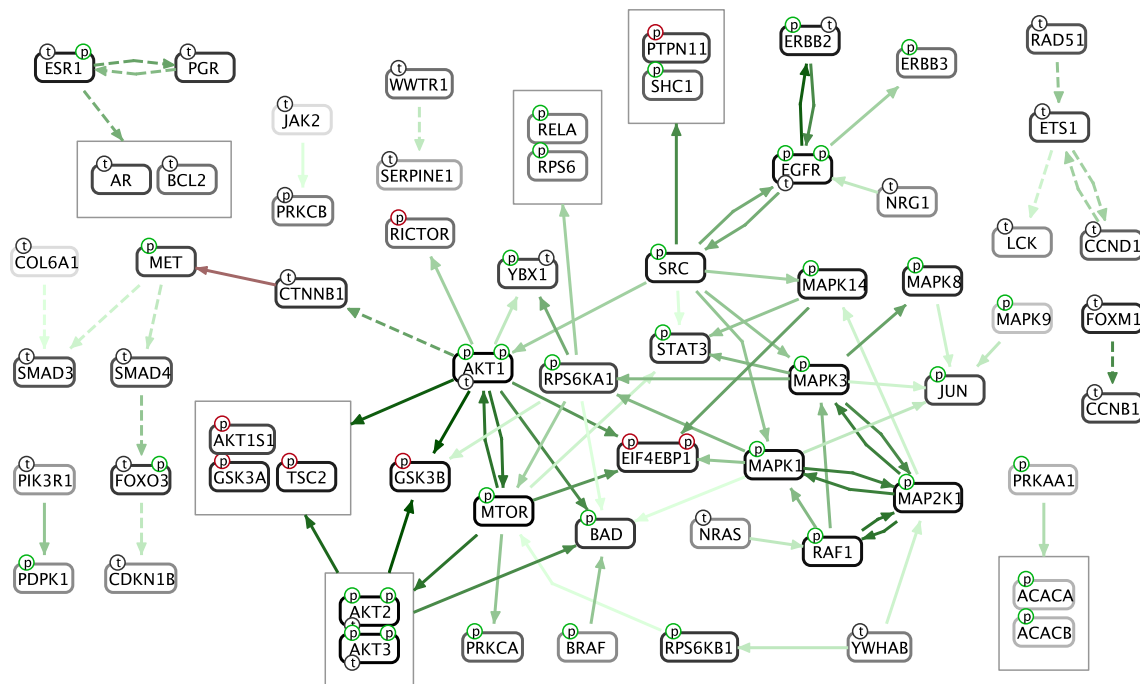


Figure 4. Recurrent results for TCGA RPPA datasets. Relations that are identified with correlation-based analysis in at least 15 cancer types are shown, where faintest color indicates 15 and boldest color indicates 30.

protein levels and their downstream (Fig. 3B). Transcriptional downstream of ESR1 captures other important transcription factors functioning in the luminal subtypes such as FOXA1, AR and PGR.

Analysis of TCGA RPPA datasets

There are 32 TCGA projects that provide proteomic and phosphoproteomic measurements with RPPA using over 200 antibodies. The low number of proteins in the datasets prevents a comprehensive pathway analysis, but the antibodies are selected for the proteins' relevancy to cancer in general and they are typically well studied with many established relations between them. We sought to determine which of these relations most frequently have evidence in the form of correlation across cancer types. We generated a correlation-based causal network for each cancer type using an FDR threshold of 0.001, then we ranked these relations according to how many cancer datasets they can explain (Fig. 4). We found that AKT to GSK3 signaling is the most frequently observed relation, detectable in 30 cancer types, followed by other downstream proteins of AKT including MTOR. Relations between several MAPK signaling proteins, and EGFR to ERBB2 signaling are also among those observed in the vast majority of cancer types. The results do not indicate that these signaling paths are almost always active in cancers, but they indicate that there is almost always a variation in their activity. This is consistent with many studies reporting AKT pathway as a major resistance mechanism to chemotherapy and some other targeted therapies^{36–38}.

Discussion

CausalPath is a novel method to aid researchers in understanding experimental observations using known mechanisms with a focus on post-translational modifications. Experimental data reveal protein features that change in coordination, and CausalPath automates the search for causal explanations in the literature. The identified relations are not certainty but hypotheses that can be used for discovery, as we have demonstrated in the platelet study.

Pathway relations come from experiments performed in highly varied contexts, such as a tissue type, a cell line, gender, or a disease. These relations' applicability to other contexts is largely unknown, and we are not capable of testing every relation in every context. The approach we present here flattens the pathway data by ignoring the context, then uses proteomic data to select a portion of relations that can explain it. In a way, we let the proteomic data define the context.

Our results show that known phosphorylation controls are more consistently observed in the proteomic data compared to known expressional controls. In the ovarian and breast cancer datasets, the size of the resulting phosphorylation networks dramatically decreases with data label shuffling while expression networks remains similar. In the recurrence study with TCGA RPPA datasets, 34% of the resulting phosphorylation controls recur in at least 15 cancer types. This ratio is only 7%

for expressional controls. For this reason, we focused more on phosphorylation relations than expressional relations in the result section. A phosphorylation relation can directly explain a phosphopeptide change, while an expressional control cannot directly explain a total protein change. The latter requires an mRNA change of the target that needs to sequentially cause the proteomic change. While we observe that mRNA and total protein measurements of the same gene are correlated in general (Supplementary Fig. 5), they are obviously not correlated enough to use protein data as a reliable proxy for mRNA.

One major limiting factor in this analysis is the large number of protein phosphorylation sites whose functions are not known, hence, their downstream cannot be included in the causality network. We have plans to mine this data from literature using natural language processing tools, but in the meantime, CausalPath reports those sites with unknown effect which also have significant change at their signaling downstream. Users have the option to review this list of modification sites and manually curate them to increase the coverage of the analysis.

Rarely, in the causality analysis results, we encounter relations that are wrong. These are generally results of faulty manual curation from literature. In these cases, we report them to the source databases, and we remove these erroneous pathway interactions from our network so that future analyses are not affected. We encourage the users to report such errors to us if they come across any.

Methods

Significance for proteomic data change and correlation

For comparison-based analyses we used a two-tailed t-test for calculating significance, requiring presence of at least 3 samples from all compared groups. For correlation-based analyses we used Pearson correlation coefficient and its associated significance, requiring at least 5 samples in the calculation. The EGF stimulation dataset provides pre-calculated p-values for all of the pairs of time points, which we directly used in the analysis. In all calculations, we used the Benjamini-Hochberg method for controlling FDR, whenever applicable. We used 0.1 as a default FDR threshold, unless indicated otherwise.

CausalPath parameters

CausalPath is a highly parametric method, designed to explore omic datasets under various settings. Following are some important parameters to consider when using the method.

Site matching proximity threshold

Protein phosphorylation sites in the literature have to exactly match the detected site in the phosphoproteomic dataset to use in causal reasoning by default. Some users may find this too strict since there can be slight shifts in the literature, or some nearby sites of proteins are likely to be phosphorylated by the same kinase. This parameter lets the analysis allow a determined inaccuracy in site mapping to explore such cases. We used strict site-matching for all the CausalPath analyses unless indicated otherwise.

Site effect proximity threshold

The effect of the phosphorylation sites on the protein activity are curated by pathway databases, mostly by PhosphoSitePlus. We also did some small scale curation for platelet analysis, EGF stimulation analysis, and RPPA analyses. CausalPath requires exact matching of these curated site effects with the sites in the data by default, however this can be too strict because nearby sites generally tend to have similar effects. This parameter lets the analysis use a determined inaccuracy while looking up site effects. In this manuscript we always used accurate matching for site effects.

Protein focus

This parameter lets the analysis use a subset of the literature relations, focusing on the neighborhood of certain proteins indicated by their gene symbols, hence reducing the number of tested hypotheses. We used this parameter during analysis of ovarian cancer subtypes as described in the relevant section.

Generation of a data-centric causal network

CausalPath result networks are gene-centric, meaning that genes are represented with nodes, and all other measurements related to a gene are mapped on the gene's node. When a data row can map to multiple genes, however, this creates a redundancy, as we have in the RPPA analysis results. There, the AKT phospho antibody can recognize all three AKTs, so we duplicate the same data on AKT1, AKT2 and AKT3. As an alternative to this view, CausalPath can generate data-centric views where nodes represent data rows. But this view do not support mapping other available omic data onto the network, and also the relations are duplicated when more than one data of the same gene can be explained by the same relation.

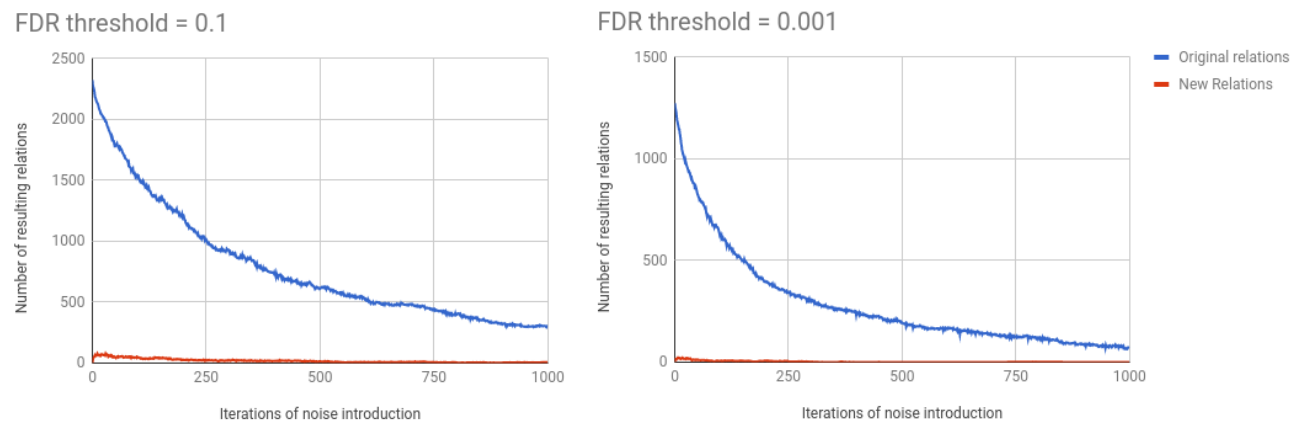


Figure 5. Robustness of CausalPath on CPTAC breast cancer dataset.

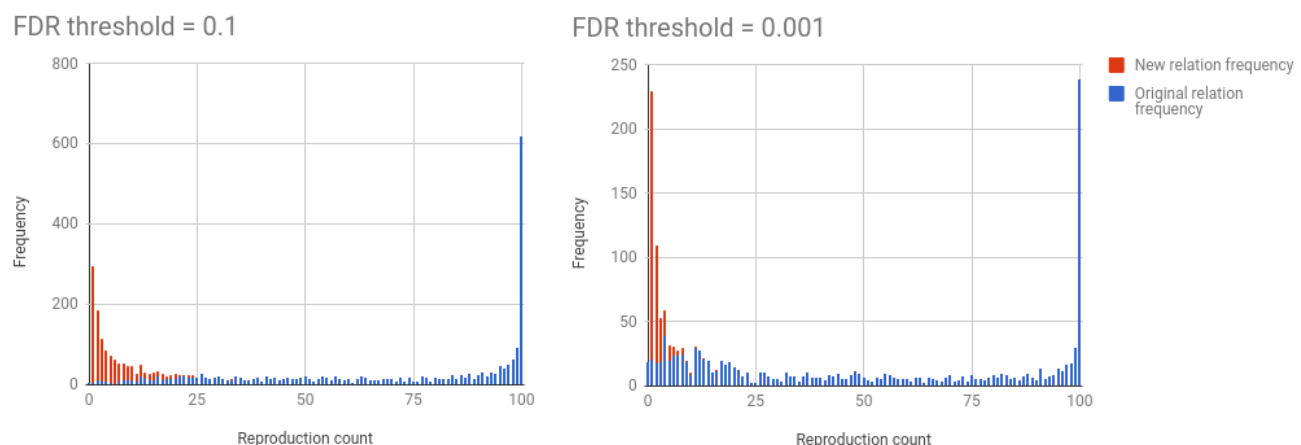


Figure 6. Reproducibility of CausalPath on CPTAC breast cancer dataset.

Protein activity

CausalPath allows users to insert their own hypotheses about protein activity changes in the case of a comparison-based analysis. The input has to be a gene symbol associated with a Boolean parameter indicating the hypothesized direction of activity change, i.e. activated or inhibited. We used this option for EGF stimulation analysis to indicate that we expect EGF to be activated because the data is only phosphoprotein, hence there is no measurable change on EGF itself to include in the analysis otherwise.

Robustness

We tested the robustness of CausalPath against noise on the CPTAC breast cancer dataset, on a correlation-based analysis with two different FDR thresholds. We iteratively introduced noise into the dataset by adding random numbers drawn from a normal distribution, and generated the causal network. At each step, we recorded the amount of the original relations as well as new relations that we have in the results (Fig. 5). Ideally, as the noise level increases, we would like the method to retain the original results and not allow the noise to generate new relations. Our tests indicate that, the original relations are sensitive to noise, which means they rapidly start decreasing in number, however, the method is safe against noise, which means we do not get many new relations due to it.

Reproducibility

We tested the reproducibility of CausalPath on the CPTAC breast cancer dataset by using random subsets of the samples, on a correlation-based analysis with two different FDR thresholds. In total of 100 trials, we used a random half of the samples at each step, and checked how frequently each causal relation is reproduced in the results (Fig. 6). The results indicate that 70% of the original relations are reproduced consistently in at least half of the trials when FDR threshold is 0.1. This ratio is reduced to 49% when we use an FDR threshold of 0.001. We observe a significant amount of new relations (red) with low reproduction counts in the tests, which are due to the accumulation of false positives from all 100 trials.

Previously published methods for pathway analysis of proteomic datasets

There is no method comparable to CausalPath for its ability to identify causal relations from pathway databases that can explain given proteomic datasets. But there are methods developed for other forms of pathway analysis for proteomics. Below is a short survey of these methods.

pCHIPS⁵

This is a network propagation method for proteomic and other data, based on the TieDIE³⁹ algorithm, where the purpose is to link differentially active kinases (indicated by proteomic data) to the differentially active transcription factors (indicated by RNAseq measurements). Proteomic changes on the kinases are propagated downstream, differential transcription factor activities are propagated upstream on the signaling network, and the overlap is identified as possible linking path(s).

While linking kinases to the transcription factors implies causality, pCHIPS does not check the conditions of causality such as if the proteomic change is indicative of activation or inhibition, or if the linking is path has a positive or a negative effect on the transcription factor activity, or their compatibility for a causality hypothesis.

PhosphoPath⁴⁰ and PTMapper⁴

Both methods are implemented as a Cytoscape plugin to visualize kinase-substrate relations on the protein-protein interaction (PPI) network. Users can run a network enrichment analysis on the PPI network for the given proteomic and other datasets, then visualize the known kinase-substrate relations on the enriched region.

PCST⁴¹

This method maps proteomic and transcriptomic data on the proteins on a weighted PPI and protein-DNA interaction network, then identifies a minimal subnetwork that connects the mapped molecules, prioritizing the most reliable connections. Authors formulate this as a prize-collecting Steiner tree (PCST) problem, and solve with a known algorithm.

PHOTON⁴²

This method maps proteomic data from a perturbation study onto the proteins on a weighted PPI network, then calculates a score for each protein based on the weighted average of the observed proteomic changes on its neighbors on the network (authors call this “functionality score” but we avoid using it as the method do not use any function-related data). The method generates a result network by connecting the perturbed protein and the proteins with high score on the PPI network.

Availability

CausalPath is freely available at <http://causalpath.org>. For an analysis, users need to provide the proteomic data in a special tab-delimited format, along with the analysis parameters. The results are displayed on the browser with the utilization of CytoscapeWeb⁴³, and the mechanistic details of the causal interactions can be viewed in SBGN-PD language, which is implemented by the utilization of SBGNViz⁴⁴. An alternative way to run CausalPath for computational biologists is from its Java sources, which is freely available at <https://github.com/PathwayAndDataAnalysis/causalpath>. The generated result networks can either be viewed by uploading to the web server or by opening with ChiBE. All network figures in this manuscript are generated with ChiBE.

Acknowledgements

This work was sponsored by DARPA under the Big Mechanism Program (Contract # W911NF-14-C-0119) and the U. S. Army Research Office (Contract # ACC-APG_RTP W911NF), and by NIH grants (U41HG006623), (GM103504) and (P41GM103504). Anil Korkut is supported by MD Anderson Cancer Center Support Grant P30 CA016672 (Bioinformatics Shared Resource). We thank to Hannah Manning and Olga Nikolova for critical reading of the manuscript. The results published here are in part based upon data generated by the TCGA Research Network: <http://cancergenome.nih.gov/>.

References

1. Duan, G. & Walther, D. The roles of post-translational modifications in the context of protein interaction networks. *PLoS Comput. Biol* **11**, e1004049 (2015).
2. Costello, J. C. *et al.* A community effort to assess and improve drug sensitivity prediction algorithms. *Nat. biotechnology* **32**, 1202–1212 (2014).
3. Korkut, A. *et al.* Perturbation biology nominates upstream–downstream drug combinations in raf inhibitor resistant melanoma cells. *Elife* **4**, e04640 (2015).
4. Narushima, Y., Kozuka-Hata, H., Tsumoto, K., Inoue, J.-I. & Oyama, M. Quantitative phosphoproteomics-based molecular network description for high-resolution kinase-substrate interactome analysis. *Bioinforma.* btw164 (2016).

5. Drake, J. M. *et al.* Phosphoproteome integration reveals patient-specific networks in prostate cancer. *Cell* **166**, 1041–1054 (2016).
6. Hill, S. M. *et al.* Inferring causal molecular networks: empirical assessment through a community-based effort. *Nat. methods* **13**, 310 (2016).
7. Triantafyllou, S. *et al.* Predicting causal relationships from biological data: Applying automated causal discovery on mass cytometry data of human immune cells. *Sci. reports* **7**, 12724 (2017).
8. Köksal, A. S. *et al.* Synthesizing signaling pathways from temporal phosphoproteomic data. *bioRxiv* (2017). DOI 10.1101/209676.
9. Suppes, P. *A probabilistic theory of causality* (North-Holland Publishing Company Amsterdam, 1970).
10. Pearl, J. Causality: models, reasoning and inference. *Econom. Theory* **19**, 46 (2003).
11. Croft, D. *et al.* The reactome pathway knowledgebase. *Nucleic acids research* **42**, D472–D477 (2014).
12. Thomas, P. D. *et al.* Panther: a library of protein families and subfamilies indexed by function. *Genome research* **13**, 2129–2141 (2003).
13. Hornbeck, P. V. *et al.* Phosphositeplus: a comprehensive resource for investigating the structure and function of experimentally determined post-translational modifications in man and mouse. *Nucleic acids research* gkr1122 (2011).
14. Romero, P. *et al.* Computational prediction of human metabolic pathways from the complete human genome. *Genome biology* **6**, R2 (2004).
15. Kanehisa, M., Furumichi, M., Tanabe, M., Sato, Y. & Morishima, K. Kegg: new perspectives on genomes, pathways, diseases and drugs. *Nucleic acids research* **45**, D353–D361 (2017).
16. Schaefer, C. F. *et al.* Pid: the pathway interaction database. *Nucleic acids research* **37**, D674–D679 (2009).
17. Demir, E. *et al.* The biopax community standard for pathway data sharing. *Nat. biotechnology* **28**, 935–942 (2010).
18. Cerami, E. G. *et al.* Pathway commons, a web resource for biological pathway data. *Nucleic acids research* **39**, D685–D690 (2011).
19. Demir, E. *et al.* Using biological pathway data with paxtools. *PLoS computational biology* **9**, e1003194 (2013).
20. Babur, Ö. *et al.* Pattern search in biopax models. *Bioinforma.* **30**, 139–140 (2014).
21. Babur, O., Dogrusoz, U., Demir, E. & Sander, C. Chibe: interactive visualization and manipulation of biopax pathway models. *Bioinforma.* **26**, 429–431 (2010).
22. Babur, Ö. *et al.* Integrating biological pathways and genomic profiles with chibe 2. *BMC genomics* **15**, 642 (2014).
23. Hu, J. *et al.* PhosphonetWORKS: a database for human phosphorylation networks. *Bioinforma.* **30**, 141–142 (2013).
24. Ross, K. E. *et al.* iptmnet: Integrative bioinformatics for studying ptm networks. *Protein Bioinformatics: From Protein Modif. Networks to Proteomics* 333–353 (2017).
25. Essaghir, A. & Demoulin, J.-B. A minimal connected network of transcription factors regulated in human tumors and its application to the quest for universal cancer biomarkers. *PloS one* **7**, e39666 (2012).
26. Babur, Ö. *et al.* Platelet procoagulant phenotype is modulated by a p38-mk2 axis regulating rtn4/nogo proximal to the endoplasmic reticulum: utility of pathway analysis. *Am. J. Physiol. Physiol.* (2018).
27. Siegel, R. L., Miller, K. D. & Jemal, A. Cancer statistics, 2016. *CA: a cancer journal for clinicians* **66**, 7–30 (2016).
28. TCGA-Network *et al.* Integrated genomic analyses of ovarian carcinoma. *Nat.* **474**, 609–615 (2011).
29. Zhang, H. *et al.* Integrated proteogenomic characterization of human high-grade serous ovarian cancer. *Cell* **166**, 755–765 (2016).
30. Mertins, P. *et al.* Proteogenomics connects somatic mutations to signalling in breast cancer. *Nat.* **534**, 55–62 (2016).
31. Chakravarty, D. *et al.* Oncokb: a precision oncology knowledge base. *JCO Precis. Oncol.* **1**, 1–16 (2017).
32. Forbes, S. *et al.* Cosmic: High-resolution cancer genetics using the catalogue of somatic mutations in cancer. *Curr. protocols human genetics* 10–11 (2016).
33. Chohan, T. A., Qian, H., Pan, Y. & Chen, J.-Z. Cyclin-dependent kinase-2 as a target for cancer therapy: progress in the development of cdk2 inhibitors as anti-cancer agents. *Curr. medicinal chemistry* **22**, 237–263 (2015).

34. Asghar, U., Witkiewicz, A. K., Turner, N. C. & Knudsen, E. S. The history and future of targeting cyclin-dependent kinases in cancer therapy. *Nat. reviews Drug discovery* **14**, 130–146 (2015).
35. Igea, A. & Nebreda, A. R. The stress kinase p38 α as a target for cancer therapy. *Cancer research* **75**, 3997–4002 (2015).
36. Cassinelli, G. *et al.* Targeting the akt kinase to modulate survival, invasiveness and drug resistance of cancer cells. *Curr. medicinal chemistry* **20**, 1923–1945 (2013).
37. Jacobsen, K. *et al.* Convergent akt activation drives acquired egfr inhibitor resistance in lung cancer. *Nat. communications* **8**, 410 (2017).
38. West, K. A., Castillo, S. S. & Dennis, P. A. Activation of the pi3k/akt pathway and chemotherapeutic resistance. *Drug resistance updates* **5**, 234–248 (2002).
39. Paull, E. O. *et al.* Discovering causal pathways linking genomic events to transcriptional states using tied diffusion through interacting events (tiedie). *Bioinforma.* **29**, 2757–2764 (2013).
40. Raaijmakers, L. M. *et al.* Phosphopath: Visualization of phosphosite-centric dynamics in temporal molecular networks. *J. proteome research* **14**, 4332–4341 (2015).
41. Huang, J. *et al.* Control of anther cell differentiation by the small protein ligand tpd1 and its receptor ems1 in arabidopsis. *PLoS Genet.* **12**, e1006147 (2016).
42. Rudolph, J. D., de Graauw, M., van de Water, B., Geiger, T. & Sharan, R. Elucidation of signaling pathways from large-scale phosphoproteomic data using protein interaction networks. *Cell systems* **3**, 585–593 (2016).
43. Lopes, C. T. *et al.* Cytoscape web: an interactive web-based network browser. *Bioinforma.* **26**, 2347–2348 (2010).
44. Sari, M. *et al.* Sbgviz: a tool for visualization and complexity management of sbgn process description maps. *PloS one* **10**, e0128985 (2015).